Mecánica Computacional Vol. XXIII, pp. 5-26
G.Buscaglia, E.Dari, O.Zamonsky (Eds.)
Bariloche, Argentina, November 2004

FINITE ELEMENT APPROXIMATION OF THERMAL MODELS FOR LOW SPEED FLOWS

Ramon Codina, Javier Principe† and Guillaume Houzeaux

International Center for Numerical Methods in Engineering (CIMNE)
Universitat Politècnica de Catalunya
Jordi Girona 1-3, Edifici C1, 08034 Barcelona, Spain
e-mail: ramon.codina@upc.es, principe@cimne.upc.es, houzeaux@cimne.upc.es
web page: http://www.cimne.com/cfdgroup

Key Words: Low Mach number models, Boussinesq approximation, linearization, stabilized finite element methods.

Abstract.

Thermally coupled low speed flows have been traditionally modeled by the incompressible Boussinesq approximation. Its relationship with models obtained from the zero Mach limit of the general compressible Navier-Stokes equations is a subject that still deserves interest, both from the conceptual and the numerical points of view. On the one hand, the way to justify the Boussinesq model by using asymptotic expansions is not unique. Several geometrical and/or thermodynamic assumptions may be used. On the other hand, numerical experiments can serve as a virtual laboratory to test the validity of the Boussinesq approach in terms of the temperature gradients present in the flow.

In this work we discuss the relationship between the Boussinesq model and asymptotic models for thermally coupled low Mach number flows, trying to clarify their connections. Likewise, we propose a finite element approximation for these models using stabilization to treat cases dominated by convection and allowing equal interpolation for all the variables. The numerical formulation is based on the subgrid scale concept.

Both in the description of the thermal models and in the presentation of the stabilized finite element techniques we employ to approximate them, our intention is to introduce *these subjects rather than to present the latest research results in these fields.*

† Supported by the *Departament d'Universitats Recerca i Societat de la Informaci ó*, Generalitat de Catalunya

1 INTRODUCTION

Several flows of interest can be considered as incompressible. This assumption is useful as it makes the problem much simpler than if a full compressible flow is considered. The compressible flow equations have different structure depending on the Mach number. If the Mach number is of the order of or greater than one, shock waves may be present. A number of issues have to be considered when solving compressible flows, such as the set of variables to be used and the prediction of such shock waves. In the incompressible case the system of equations is smaller and shocks as well as sound waves are absent. Furthermore, the mathematical structure of incompressible equations is much better understood.

However many important flows cannot be considered as incompressible due to the presence of thermal effects. In this work low speed flows (flows with a low Mach number) will be considered and two simplified models will be presented: the zero Mach number model and the Boussinesq approximation. These models have a common characteristic that makes them attractive, namely, they do not admit sound waves solutions. The purpose of this work is to clarify the connection between these models and to develop a stabilized finite element model to approximate them.

When heat exchange is taken into account, the zero Mach number limit leads to a splitting of the pressure into a constant-in space thermodynamic contribution and a mechanical one. This limits removes the acoustic modes and the flow behaves as incompressible (in the sense that pressure is determined by the mass conservation equation and not by the state equation) but large variations of density due to temperature variations are allowed. This limit has been studied first in the inviscid case,[1] and later generalized to the viscous case.[2] Then, a rigorous derivation including combustion was presented[3] and recently the numerical implications of this limit have been studied.[4,5]

The Boussinesq approximation, that consists in ignoring variations of density except where they multiply the gravity acceleration, has shown to be valid for a thin layer of fluid.[6] However, the usual argument to retain small density variations in the forcing term of the momentum equation is based on physical arguments and not on a limiting process. The first attempt to present a rigorous derivation of the Boussinesq approximation was performed by Mihaljan.[7] A two parameter expansion of the full compressible equations was proposed and the Boussinesq approximation was found to the lowest order in both ε_1 and ε_2, the parameters of the expansion. Several problems of this approach were found:[8] the two parameters introduced by Mihaljan are of order $\varepsilon_1 \sim 10^{-4}$ and $\varepsilon_2 \sim 10^{-11}$ indicating that a second order approximation for ε_1 has the same order as ε_2. The Mihaljan approach was improved by Perez Cordon and Velarde.[8] The new ingredient was the selection of an appropriate reference state. A derivation of the Boussinesq equations taking a reference state into account and allowing temperature and pressure dependent properties was presented by Gray and Giorgini.[9] We note that all these works are concerned with natural convection problems.

An asymptotic justification of the Boussinesq approximation was developed in the works of Zeytounian[10–12] and Bois.[13,14] These developments dealt first with polytropic gases[10,13] and the

main conclusion was that the Mach number is a small parameter in the Boussinesq approximation and that the approximation is found in the limit between the quasi-static and the anelastic approximations. The quasi-static approximation is one in which the vertical velocity is fixed (to zero in ideal fluids) to satisfy an hydrostatic balance allowing plane motions only. The anelastic approximation has been used for a long time in the context of atmospheric flows.[15,16] This approximation removes the height limitation present in the Boussinesq's one.

Apart from the discussion of the physical model, in this work we also present its finite element approximation by using a stabilized finite element method. The goal is to cope with the numerical instabilities found when convection dominates (that is, the local Reynolds and Péclet numbers are high) and also when the pressure and velocity interpolations are the same. These are two classical sources of numerical instabilities. Our purpose is to summarize the formulation we have been using in several flow problems applied to the particular case considered here.

The paper is organized as follows. In Section 2 we describe the physics of the problems, whereas in Section 3 we present the numerical approximation of the stationary problem, considering both the space discretization and the linearization. In Section 4 we present the numerical results we have obtained for a classical benchmark problem and finally we close with some conclusions in Section 5.

2 PHYSICAL MODEL

2.1 Navier-Stokes equations

The equations that describe the dynamics of a compressible flow are the mass, momentum and energy conservation plus a state equation relating the thermodynamic variables. They read

$$\begin{aligned}\frac{\mathrm{D}\rho}{\mathrm{D}t} &= -\rho\nabla\cdot\boldsymbol{u},\\ \rho\frac{\mathrm{D}\boldsymbol{u}}{\mathrm{D}t} &= \nabla\cdot\boldsymbol{\sigma}+\rho\boldsymbol{g},\\ \rho\frac{\mathrm{D}e}{\mathrm{D}t} &= -\nabla\cdot\boldsymbol{q}+\boldsymbol{\sigma}:\boldsymbol{\varepsilon}(\boldsymbol{u})+Q.\end{aligned}$$

Here $\boldsymbol{u}$ is the velocity, ρ the density, p the pressure, e the internal energy, $\boldsymbol{g}$ and Q are the external force and energy source, respectively; $\boldsymbol{q}$ is the heat flux and $\boldsymbol{\sigma}$ the stress tensor related to the (rate of) deformation tensor (symmetric part of the velocity gradient, $\boldsymbol{\varepsilon}(\boldsymbol{u}) = \frac{1}{2}\left(\nabla\boldsymbol{u}+\nabla\boldsymbol{u}^T\right)$) through the following constitutive equations

$$\boldsymbol{\sigma} = -p\boldsymbol{I}+2\mu\boldsymbol{\varepsilon}'(\boldsymbol{u}), \quad \boldsymbol{q} = -k\nabla\theta,$$

where θ is the temperature, k and μ are the conductivity and viscosity, $\boldsymbol{I}$ the identity tensor and $\boldsymbol{\varepsilon}'(\boldsymbol{u}) = \boldsymbol{\varepsilon}-\frac{1}{3}\nabla\cdot\boldsymbol{u}\boldsymbol{I}$ the deviatoric part of the deformation tensor. Note that the Stokes hypothesis is used, although this is not essential.

Using equilibrium thermodynamics the system can be written as

$$
\begin{aligned}
\frac{\mathrm{D}\rho}{\mathrm{D}t} + \rho\nabla\cdot\boldsymbol{u} &= 0,\\
\rho\frac{\mathrm{D}\boldsymbol{u}}{\mathrm{D}t} + \nabla p &= \nabla\cdot(2\mu\boldsymbol{\varepsilon}'(\boldsymbol{u})) + \rho\boldsymbol{g},\\
\rho c_p\frac{\mathrm{D}\theta}{\mathrm{D}t} - \beta\theta\frac{\mathrm{D}p}{\mathrm{D}t} &= \nabla\cdot(k\nabla\theta) + \Phi + Q,\\
\rho &= F\left(p,\theta\right),
\end{aligned}
\tag{1}
$$

where β is the thermal expansion coefficient, c_p the constant pressure specific heat and Φ is the Rayleigh dissipation function, given by $\Phi = 2\mu\boldsymbol{\varepsilon}'(\boldsymbol{u}) : \boldsymbol{\varepsilon}'(\boldsymbol{u})$.

2.2 Dimensionless equations

Considering scales of length (l_0), time (t_0), density (ρ_0), pressure (p_0), temperature (θ_0), velocity (u_0), viscosity (μ_0), conductivity (k_0), specific heat (c_{p_0}), force (g_0) and energy (Q_0) we have the following dimensionless numbers: Strouhal ($S = l_0/u_0t_0$), Mach ($M = u_0/\sqrt{p_0/\rho_0}$), Reynolds ($Re = \rho_0u_0l_0/\mu_0$), Péclet ($Pe = \rho_0c_pu_0l_0/k_0$), Froude ($F = u_0/\sqrt{g_0l_0}$) and a heat release number ($H = t_0Q_0/\rho_0c_{p_0}\theta_0$), that is a measure of the power of the heat source. The dimensionless equations are (without using any distinctive notation for them):

$$
\begin{aligned}
S\frac{\partial\rho}{\partial t} + \nabla\cdot(\rho\boldsymbol{u}) &= 0,\\
S\rho\frac{\partial\boldsymbol{u}}{\partial t} + \rho\boldsymbol{u}\cdot\nabla\boldsymbol{u} + \frac{1}{M^2}\nabla p &= \frac{1}{Re}\nabla\cdot(2\mu\boldsymbol{\varepsilon}'(\boldsymbol{u})) + \frac{1}{F^2}\rho\boldsymbol{g},\\
S\rho c_p\frac{\partial\theta}{\partial t} + \rho c_p\boldsymbol{u}\cdot\nabla\theta - S_t\beta\theta\left(S\frac{\partial p}{\partial t} + \boldsymbol{u}\cdot\nabla p\right) &= \frac{M^2}{Re}\Phi + \frac{1}{Pe}\nabla\cdot(k\nabla\theta) + HSQ,\\
\rho &= F(p,\theta).
\end{aligned}
\tag{2}
$$

The parameter S_t depends on the state equation and is given by

$$
S_t = \frac{p_0}{\rho_0c_{p_0}\theta_0} = \frac{p_0}{F\left(p_0,\theta_0\right)c_{p_0}\theta_0}.
$$

For an ideal gas the state equation reduces to $p = \rho\theta$ and the parameter S_t to $S_t = \gamma - 1/\gamma$.

2.3 Low Mach number asymptotics

2.3.1 Single scale approximation

The limit when the Mach number goes to zero can be found using standard procedures of asymptotic analysis.[17] The first step is to expand all flow variables in power series of the Mach number as

$$
\xi\left(\boldsymbol{x},t,M\right) = \sum_{i=0}^{n} M^i\xi^i\left(\boldsymbol{x},t\right) + o(M^n),
$$

for $\xi = \boldsymbol{u}$, $\xi = p$, $\xi = \rho$, $\xi = \theta$. The second step is to substitute them into the dimensionless equations (2) and to require that all terms in the expanded equations that are multiplied by the same power of the Mach number vanish. Then a hierarchy of equations that follows is obtained.

The momentum conservation equation gives

$$
\begin{aligned}
&\wr(M^0): && \nabla p^0 = 0,\\
&\wr(M^1): && \nabla p^1 = 0,\\
&\wr(M^2): && \rho^0 \frac{\partial \boldsymbol{u}^0}{\partial t} + \rho^0 \boldsymbol{u}^0 \cdot \nabla \boldsymbol{u}^0 + \nabla p^2 = \frac{1}{Re} \nabla \cdot \left(2\mu \boldsymbol{\varepsilon}'(\boldsymbol{u}^0)\right) + \frac{1}{F^2} \rho^0 \boldsymbol{g}.
\end{aligned}
$$

The first two equations give $p^0 = p^0(t)$ and $p^1 = p^1(t)$. This is a very important result. The pressure splits into three contributions: p^0 a reference thermodynamic pressure, p^1 an acoustic component and p^2 a mechanical pressure. The first one, constant over the whole domain, changes its value only by global heating or mass adding. The acoustic pressure p^1 only appears if one considers low but finite Mach number giving rise to acoustic effects.[4,5] The mechanical pressure component p^2 is determined from a velocity constraint and not by the state equation, playing the same role as in the incompressible equations.

In the zero Mach number limit a system of equations for ρ^0, θ^0, p^2 and $\boldsymbol{u}^0$ has to be solved. The reference pressure p^0 is determined from a global equation as presented in the following subsection. The system to be solved is given by

$$
\begin{aligned}
\frac{\partial \rho^0}{\partial t} + \nabla \cdot \left(\rho^0 \boldsymbol{u}^0\right) &= 0,\\
\rho^0 \frac{\partial \boldsymbol{u}^0}{\partial t} + \rho^0 \boldsymbol{u}^0 \cdot \nabla \boldsymbol{u}^0 + \nabla p^2 &= \frac{1}{Re} \nabla \cdot \left(2\mu \boldsymbol{\varepsilon}'(\boldsymbol{u}^0)\right) + \frac{1}{F^2} \rho^0 \boldsymbol{g},\\
\rho^0 c_p^0 \frac{\partial \theta^0}{\partial t} + \rho^0 c_p^0 \boldsymbol{u} \cdot \nabla \theta^0 - S_t \beta^0 \theta^0 \frac{\mathrm{d}p^0}{\mathrm{d}t} &= \frac{1}{Pe} \nabla \cdot \left(k \nabla \theta^0\right) + HSQ,
\end{aligned}
\tag{3}
$$

and a state equation of the form $\rho^0 = F\left(p^0, \theta^0\right)$, that for an ideal gas gives

$$
p^0 = \rho^0 \theta^0. \tag{4}
$$

2.3.2 Determination of the reference pressure

As the reference thermodynamic pressure is constant in space, it can be determined by a global balance. Starting from the zeroth order expansion of the mass, energy and state equations (3), a constraint for the velocity can be obtained. In the case of an ideal gas it reads

$$
p^0 \nabla \cdot \boldsymbol{u}^0 = -\frac{1}{\gamma} \frac{\mathrm{d}p^0}{\mathrm{d}t} + \frac{1}{Pe} \nabla \cdot \left(k \nabla \theta^0\right) + HSQ. \tag{5}
$$

This equation, integrated over the domain gives an ordinary differential equation for the reference pressure. In general this equation will be an implicit equation for p^0, but in the case of an

ideal gas it is explicitly given by

$$p^0 \int_{\partial\Omega} \boldsymbol{u}^0 \cdot \boldsymbol{n} = -\frac{V_\Omega}{\gamma}\frac{\mathrm{d}p^0}{\mathrm{d}t} + \frac{1}{Pe}\int_{\partial\Omega} \boldsymbol{q}\cdot\boldsymbol{n} + HS\int_\Omega Q,$$

where $V_\Omega = \text{meas}(\Omega)$. It is observed that the mean constant-in-space thermodynamic pressure changes in time due to the addition or subtraction of mass (left hand side term) or to heat addition or subtraction either by the contour (second right hand side term) or by volumetric sources (last right hand side term).

2.3.3 Multiple scale approximation

The multiple scale analysis of the zero Mach number limit reveals the role of acoustic effects. An outline of this type of approximation will be presented here. The details can be found in the literature.[4,5,17] In this type of approximations, to face a problem that presents different scales a new variable that represents such scales is introduced. In the case of a flow that presents acoustic effects a new time scale of the form $\tau = t/M$ is introduced.[5] This new variable represents a very short time scale compared to the time scale given by the variable t. Another possibility[4] is to introduce a new space scale of the form $\boldsymbol{\zeta} = M\boldsymbol{x}$. Then, an expansion of the unknowns in terms of both scales reads

$$\xi\left(\boldsymbol{x}, t, M\right) = \sum_{i=0}^{n} M^i \xi^i\left(\boldsymbol{x}, \tau, t\right) + o(M^n),$$

and we have

$$\left.\frac{\partial}{\partial t}\right|_M = \frac{\partial}{\partial t} + \frac{1}{M}\frac{\partial}{\partial \tau}. \tag{6}$$

As in the case of a single scale analysis, introducing this expansion into equations (1) a hierarchy of equations is obtained. It is important to remark that because of the implicit dependence of the different terms on the Mach number through the new time scale, is not obvious that we can require each term in the expansion to vanish, but this is actually the case.[18] From each equation in this hierarchy it can be deduced that the zeroth order density, temperature and pressure do not depend on the fast time scale τ. Also, the following evolution equations for the first order pressure is obtained

$$\frac{\partial^2 p^1}{\partial \tau^2} - \nabla\cdot\left(c_0^2 \nabla p^1\right) = \gamma HS\frac{\partial Q}{\partial \tau}, \tag{7}$$

where

$$c_0^2 = \gamma\frac{p^0\left(t\right)}{\rho^0\left(\boldsymbol{x}, t\right)},$$

does not depend on τ.

Equation (7) is a wave equation for the first order pressure that shows the dependence of the first order pressure on the fast time scale τ (acoustic effects) which is determined by the time dependence of the heat source on the fast time scale. A tempting conclusion is that if the heat source varies slowly (i.e. independently of the fast time scale τ) acoustic effects will be absent but this conclusion is false because sound can be generated by the flow itself. This fact is well known after the development of the acoustic analogy by Lighthill.[19] Even in absence of a rapidly variable heat source, in a low but finite Mach number regime, $\boldsymbol{u}^0$ and p^2 will give rise to a dependence of the second order density on the fast time scale, so for finite Mach number all the terms in the expansion remain coupled even for slow external heating.[4,5]

2.4 Boussinesq model

The low Mach number approximation developed in the previous section was carried out considering all the dimensionless numbers, except the Mach number, fixed. In this section the possibility of a low Froude number is taken into account and the Boussinesq model is presented. As previously mentioned, successive improvements of the derivation of the Boussinesq approximation have been made introducing a reference state about which a perturbative scheme is developed.[8,9] Following the ideas of Bois and Zeytounian[10–14] we next present some arguments for the choice of such state. As we will consider a vanishing Froude number, it is useful to introduce the Boussinesq number, defined as

$$B = \frac{\rho_0 g l_0}{p_0} = \frac{M^2}{F^2}.$$

This number was defined first by Zeytounian[10] but its importance in verticaly stratified flows was already noted previously.[15] As both M and F are low, the Boussinesq number can be finite or zero depending on the relation between F and M. The external force will be considered due to gravity and supposed in the $(-\hat{\boldsymbol{z}})$ direction. Then a single scale expansion on powers of the Mach number of the equations (1) will give, to the first order in the momentum equation

$$\nabla p^0 = -B\rho^0 \hat{\boldsymbol{z}}$$

from where it follows that

$$p^0 = p^0\left(z,t\right), \quad \rho^0 = \rho^0\left(z,t\right), \quad \theta^0 = \theta^0\left(z,t\right).$$

We will consider this reference state as independent of time.[10–14] The possibility of this assumption depends on the boundary conditions of the problem studied. In an unbounded domain, one can think of flow at infinity that only depends on z.[13] Under this assumption the lowest order energy equation is given by

$$w^0\rho^0\left(\frac{\mathrm{d}\theta^0}{\mathrm{d}z} + BS_t\beta^0\theta^0\hat{\boldsymbol{z}}\right) = \frac{1}{Pe}\frac{\mathrm{d}}{\mathrm{d}z}\left(k\frac{\mathrm{d}\theta^0}{\mathrm{d}z}\right) + HSQ. \tag{8}$$

Several different cases need to be considered in the zero Mach number limit of this equation. First one notes that, if the term

$$\frac{\mathrm{d}\theta^0}{\mathrm{d}z} + BS_t\beta^0\theta^0\hat{\boldsymbol{z}} = \wr(1),$$

then from equation (8) one obtains

$$w^0 = \frac{\frac{1}{Pe}\frac{\mathrm{d}}{\mathrm{d}z}\left(k\frac{\mathrm{d}\theta^0}{\mathrm{d}z}\right) + HSQ}{\rho^0\frac{\mathrm{d}\theta^0}{\mathrm{d}z} - S_t\beta^0\theta^0\frac{\mathrm{d}p^0}{\mathrm{d}z}}$$

that for an ideal fluid in absence of external heating gives $w^0 = 0$. This case is called the quasi-static approximation.[10–14]The vertical velocity is constrained by an hydrostatic equilibrium in the vertical direction and only plane motions can occur.

A different situation occurs if

$$\frac{\mathrm{d}\theta^0}{\mathrm{d}z} + BS_t\beta^0\theta^0\hat{\boldsymbol{z}} = \wr(M), \tag{9}$$

as in this case the constraint for the vertical velocity disappears. The relation (9) will be valid if $B \to 0$ and $\frac{\mathrm{d}\theta^0}{\mathrm{d}z} \to 0$. In this case θ^0 can only be constant or depend on a slow variable $\zeta = Bz$. Then we consider an asymptotic expansion of the form[10–14]

$$\xi\left(\boldsymbol{x}, t, M\right) = \xi^0\left(\zeta\right) + \sum_{i=1}^{n} M^i\xi^i\left(\boldsymbol{x}, t\right) + o(M^n), \tag{10}$$

for $\xi = p$, $\xi = \rho$, $\xi = \theta$ and

$$\boldsymbol{u}\left(\boldsymbol{x}, t, M\right) = \sum_{i=0}^{n} M^i\boldsymbol{u}^i\left(\boldsymbol{x}, t\right) + o(M^n). \tag{11}$$

Introducing (10) and (11) in the dimensionless equations (1) it follows that p^1 is a constant ($p^1 = 0$ can be taken). If one assumes that the heat source is weak (i.e. the heat release number goes to zero as the Mach number) the Boussinesq equations are obtained

$$\nabla\cdot\boldsymbol{u}^0 = 0,$$
$$\rho^0\frac{\partial\boldsymbol{u}^0}{\partial t} + \rho^0\boldsymbol{u}^0\cdot\nabla\boldsymbol{u}^0 + \nabla p^2 = \frac{1}{Re}\nabla\cdot\left(2\mu\boldsymbol{\varepsilon}'(\boldsymbol{u}^0)\right) - \rho^1\hat{\boldsymbol{z}},$$
$$\rho^0\frac{\partial\theta^1}{\partial t} + \rho^0\boldsymbol{u}^0\cdot\nabla\theta^1 + \boldsymbol{u}^0\cdot\hat{\boldsymbol{z}}\left(\frac{\mathrm{d}\theta^0}{\mathrm{d}\zeta} - S_t\beta^0\theta^0\frac{\mathrm{d}p^0}{\mathrm{d}\zeta}\right) = \frac{1}{Pe}\nabla\cdot\left(k\nabla\theta^0\right) + HSQ.$$

At a first sight there is an extra term in the energy equation proportional to the vertical velocity. This term is also found in the literature.[6,8–14] Under certain conditions this term can be

neglected.[9] A state equation has to be considered to evaluate ρ^1. If we consider an ideal gas we have

$$\wr(M^0): \qquad p^0 = \rho^0\theta^0, \tag{12}$$
$$\wr(M^1): \qquad 0 = \rho^1 + \theta^1. \tag{13}$$

For a general variation of density as function of temperature and pressure, a first order expansion about θ_0 and p_0 is considered. We have (in dimensionless form)

$$\rho = \left[1 - \beta_0\left(\theta - 1\right) + K_0\left(p - 1\right)\right].$$

Then

$$\wr(M^0): \qquad \rho^0 = \left[1 - \beta_0\left(\theta^0 - 1\right) + K_0\left(p^0 - 1\right)\right], \tag{14}$$
$$\wr(M^1): \qquad \rho^1 = -\beta_0\theta^1, \tag{15}$$

so in any case a linear relation between temperature and density is found.

3 NUMERICAL APPROXIMATION

In this section we present the numerical approximation of both the low Mach number and the Boussinesq *stationary* problems. In the numerical examples presented in Section 4, we solve directly the stationary form of the problem by performing nonlinear iterations with a linearization technique described later.

The two problems considered can be written in a unified manner as a system of nonlinear convection-diffusion-reaction equations of the form

$$\mathcal{L}(\boldsymbol{U};\boldsymbol{U}) \;=\; \boldsymbol{F} \;\text{ in }\; \Omega, \tag{16}$$

where

$$\mathcal{L}(\boldsymbol{U}_0;\boldsymbol{U}) \;:=\; \boldsymbol{A}_i(\boldsymbol{U}_0)\frac{\partial \boldsymbol{U}}{\partial x_i} - \frac{\partial}{\partial x_i}\left(\boldsymbol{K}_{ij}\frac{\partial \boldsymbol{U}}{\partial x_j}\right) + \boldsymbol{S}(\boldsymbol{U}_0)\boldsymbol{U}. \tag{17}$$

Equation (16) needs to be supplied with appropriate boundary conditions. There, Ω is the computational domain, $\boldsymbol{U} = (\boldsymbol{u}, p, \theta)$, $\boldsymbol{F}$ is a known vector of $n_{\rm unk} = n_{\rm sd} + 2$ components and $\boldsymbol{A}_i$, $\boldsymbol{K}_{ij}$ and $\boldsymbol{S}$ are $n_{\rm unk} \times n_{\rm unk}$ matrices ($i, j = 1, ..., n_{\rm sd}$). The usual summation convention is implied in (16), with indices running from 1 to the number of space dimensions $n_{\rm sd}$. We shall refer to the terms of the left-hand-side (LHS) of this equation as the convective, the diffusive and the reactive term.

The matrices and vectors involved in (16) may depend on the unknown $\boldsymbol{U}$. Their expression is, in the two-dimensional case ($n_{\rm sd} = 2$):

Low Mach number model:

$$\boldsymbol{K}_{ij} = \begin{bmatrix} \mu\delta_{ij} + \mu\delta_{i1}\delta_{j1} + \frac{2\mu}{3}\delta_{i1}\delta_{j1} & \mu\delta_{i2}\delta_{j1} + \frac{2\mu}{3}\delta_{i1}\delta_{j2} & 0 & 0 \\ \mu\delta_{i1}\delta_{j2} + \frac{2\mu}{3}\delta_{i2}\delta_{j1} & \mu\delta_{ij} + \mu\delta_{i2}\delta_{j2} + \frac{2\mu}{3}\delta_{i2}\delta_{j2} & 0 & 0 \\ 0 & 0 & 0 & 0 \\ 0 & 0 & 0 & k \end{bmatrix},$$

$$\boldsymbol{A}_i(\boldsymbol{U}) = \begin{bmatrix} \rho u_i & 0 & \delta_{i1} & 0 \\ 0 & \rho u_i & \delta_{i2} & 0 \\ \delta_{i1} & \delta_{i2} & 0 & -\frac{1}{\theta}u_i \\ 0 & 0 & 0 & \rho u_i \end{bmatrix}, \quad \boldsymbol{S}(\boldsymbol{U}) = \begin{bmatrix} 0 & 0 & 0 & \rho g_1 \\ 0 & 0 & 0 & \rho g_2 \\ 0 & 0 & 0 & 0 \\ 0 & 0 & 0 & 0 \end{bmatrix}, \quad \boldsymbol{F} = \begin{bmatrix} 0 \\ 0 \\ 0 \\ Q \end{bmatrix},$$

where the density ρ depends on the temperature θ through the relation $\rho = p_{\rm th}\theta^{-1}$, $p_{\rm th}$ being the thermodynamic pressure, corresponding to p^0 in (4). Note that this relation has been used to rewrite the continuity equation (third row).

Boussinesq model:

$$\boldsymbol{K}_{ij} = \begin{bmatrix} \mu\delta_{ij} & 0 & 0 & 0 \\ 0 & \mu\delta_{ij} & 0 & 0 \\ 0 & 0 & 0 & 0 \\ 0 & 0 & 0 & k \end{bmatrix}, \quad \boldsymbol{A}_i(\boldsymbol{U}) = \begin{bmatrix} \rho u_i & 0 & \delta_{i1} & 0 \\ 0 & \rho u_i & \delta_{i2} & 0 \\ \delta_{i1} & \delta_{i2} & 0 & 0 \\ 0 & 0 & 0 & \rho u_i \end{bmatrix},$$

$$\boldsymbol{S} = \begin{bmatrix} 0 & 0 & 0 & \rho\beta g_1 \\ 0 & 0 & 0 & \rho\beta g_2 \\ 0 & 0 & 0 & 0 \\ 0 & 0 & 0 & 0 \end{bmatrix}, \quad \boldsymbol{F} = \begin{bmatrix} \rho\beta\theta_0 g_1 \\ \rho\beta\theta_0 g_2 \\ 0 \\ Q \end{bmatrix}.$$

Note that in this case ρ is not an unknown of the problem but a physical property.

3.1 Variational problem

Let $\mathcal{W}$ be the functional space where the solution is to be sought. The components of $\boldsymbol{u}$ and θ must be $H^1(\Omega)$ functions satisfying the Dirichlet boundary conditions ($\mathcal{W}$ is thus an affine space) whereas p must be an $L^2(\Omega)$ function. Let also $\mathcal{W}_0$ be the corresponding space of test functions.

Let matrices $\boldsymbol{A}_i$ be split as $\boldsymbol{A}_i = \boldsymbol{A}_i^{\rm c} + \boldsymbol{A}_i^{\rm f}$, where $\boldsymbol{A}_i^{\rm c}$ is the part of the convection matrices which is *not* integrated by parts and $\boldsymbol{A}_i^{\rm f}$ the part that *is* integrated by parts. In our case, $\boldsymbol{A}_i^{\rm f}$ corresponds to the components of $\boldsymbol{A}_i$ that multiply the pressure. Assuming that the von Neumann conditions are of the form

$$n_i\boldsymbol{K}_{ij}\frac{\partial \boldsymbol{U}}{\partial x_j} - n_i\boldsymbol{A}_i^{\rm f}\boldsymbol{U} = \boldsymbol{T} \quad \text{on} \quad \Gamma_N \subset \partial\Omega,$$

the weak form of the problem consists in finding $\boldsymbol{U} \in \mathcal{W}$ such that

$$B(\boldsymbol{U};\boldsymbol{U},\boldsymbol{V}) - L(\boldsymbol{V}) = 0 \qquad \forall \boldsymbol{V} \in \mathcal{W}_0, \tag{18}$$

where the nonlinear form B and the linear form L are defined as

$$B(\boldsymbol{U}_0;\boldsymbol{U},\boldsymbol{V}) := \langle \boldsymbol{V}^{\mathrm{t}}, \mathcal{L}(\boldsymbol{U}_0;\boldsymbol{U})\rangle := \int_\Omega \boldsymbol{V}^{\mathrm{t}}\boldsymbol{A}_i^{\mathrm{c}}(\boldsymbol{U}_0)\frac{\partial \boldsymbol{U}}{\partial x_i}\,\mathrm{d}\Omega$$
$$-\int_\Omega \frac{\partial}{\partial x_i}\left(\boldsymbol{V}^{\mathrm{t}}\boldsymbol{A}_i^{\mathrm{f}}(\boldsymbol{U}_0)\right)\boldsymbol{U}\,\mathrm{d}\Omega + \int_\Omega \frac{\partial \boldsymbol{V}^{\mathrm{t}}}{\partial x_i}\boldsymbol{K}_{ij}\frac{\partial \boldsymbol{U}}{\partial x_j}\,\mathrm{d}\Omega + \int_\Omega \boldsymbol{V}^{\mathrm{t}}\boldsymbol{S}(\boldsymbol{U}_0)\boldsymbol{U}\,\mathrm{d}\Omega, \quad (19)$$

$$L(\boldsymbol{V}) := \int_\Omega \boldsymbol{V}^{\mathrm{t}}\boldsymbol{F}\,\mathrm{d}\Omega + \int_{\Gamma_N} \boldsymbol{V}^{\mathrm{t}}\boldsymbol{T}\,\mathrm{d}\Gamma. \quad (20)$$

The Galerkin finite element approximation of this problem is standard. If $\mathcal{W}_h$ is a finite element space to approximate $\mathcal{W}$ and $\mathcal{W}_{0,h}$ the associated test function space, the discrete problem consists in finding $\boldsymbol{U}_h \in \mathcal{W}_h$ such that

$$B(\boldsymbol{U}_h;\boldsymbol{U}_h,\boldsymbol{V}_h) - L(\boldsymbol{V}_h) = 0 \qquad \forall \boldsymbol{V}_h \in \mathcal{W}_{0,h}. \quad (21)$$

It is well known that this formulation lacks stability when the diffusive terms are small, compared either to the convective or to the reactive terms. Likewise, since the quadratic form associated to $\boldsymbol{K}_{ij}$ is not positive definite, it is not possible to use equal interpolation for all the components of $\boldsymbol{U}$. In our case, velocity-pressure pairs must satisfy the inf-sup condition. If the thermal coupling is strong, this could also lead to a source of numerical instabilities.

3.2 Stabilized finite element approximation

The purpose of this subsection is to describe the stabilized finite element formulation we employ to solve problem (18). This formulation is based on the subgrid scale method with an algebraic approximation to the subscales.[20]

Instead of dealing with the nonlinear problem, we will motivate the stabilization technique for its linearized version, that is,

$$B(\boldsymbol{U}_{0,h};\boldsymbol{U},\boldsymbol{V}) - L(\boldsymbol{V}) = 0 \qquad \forall \boldsymbol{V} \in \mathcal{W}_0, \quad (22)$$

where $\boldsymbol{U}_{0,h}$ is a known finite element function. In the linearized process described later, it will be an approximation to $\boldsymbol{U}$. The possibility of using the subgrid scale method in nonlinear problems is sketched in a recent article.[21] Both its numerical performance and its theoretical consequences need to be further explored.

3.2.1 The subgrid scale approach

Let us split the continuous space $\mathcal{W}$ as $\mathcal{W} = \mathcal{W}_h \oplus \tilde{\mathcal{W}}$, where $\tilde{\mathcal{W}}$ can be in principle any space to complete $\mathcal{W}_h$ in $\mathcal{W}$. To fix ideas, we may think of $\tilde{\mathcal{W}}$ as the orthogonal complement of $\mathcal{W}_h$ with respect to the L^2 inner product in $\mathcal{W}$. Since $\tilde{\mathcal{W}}$ represents the component of $\mathcal{W}$ which is not reproduced by the finite element space, we call it the space of subscales or subgrid scales. The continuous equation (18) can now be written as the system

$$B(\boldsymbol{U}_{0,h};\boldsymbol{U}_h,\boldsymbol{V}_h) + B(\boldsymbol{U}_{0,h};\tilde{\boldsymbol{U}},\boldsymbol{V}_h) = L(\boldsymbol{V}_h) \quad \forall \boldsymbol{V}_h \in \mathcal{W}_h, \quad (23)$$
$$B(\boldsymbol{U}_{0,h};\boldsymbol{U}_h,\tilde{\boldsymbol{V}}) + B(\boldsymbol{U}_{0,h};\tilde{\boldsymbol{U}},\tilde{\boldsymbol{V}}) = L(\tilde{\boldsymbol{V}}) \quad \forall \tilde{\boldsymbol{V}} \in \tilde{\mathcal{W}}, \quad (24)$$

where $\boldsymbol{U} = \boldsymbol{U}_h + \tilde{\boldsymbol{U}}$ and $\boldsymbol{U}_h \in \mathcal{W}_h$, $\tilde{\boldsymbol{U}} \in \tilde{\mathcal{W}}$.

Let $n_{\rm el}$ be the number of elements of the finite element partition of the domain Ω and let Ω^e be the region occupied by the e-th element. It is useful for the following to introduce the notation

$$\int_{\Omega'} := \sum_{e=1}^{n_{\rm el}} \int_{\Omega^e}, \quad \int_{\partial\Omega'} := \sum_{e=1}^{n_{\rm el}} \int_{\partial\Omega^e}. \tag{25}$$

Let us assume that the solution of the continuous problem $\boldsymbol{U}$ is smooth. Integrating by parts within each element domain it is found that problem (23)-(24) can be written as

$$\begin{aligned} B(\boldsymbol{U}_{0,h};\boldsymbol{U}_h,\boldsymbol{V}_h) &+ \int_{\partial\Omega'} \tilde{\boldsymbol{U}}^{\rm t} n_i \left(\boldsymbol{K}_{ij}\frac{\partial \boldsymbol{V}_h}{\partial x_j} - \boldsymbol{A}_i^{\rm f}\boldsymbol{V}_h \right) {\rm d}\Gamma \\ &+ \int_{\Omega'} \tilde{\boldsymbol{U}}^{\rm t} \mathcal{L}^*(\boldsymbol{U}_{0,h};\boldsymbol{V}_h)\,{\rm d}\Omega = L(\boldsymbol{V}_h), \end{aligned} \tag{26}$$

$$\begin{aligned} \int_{\partial\Omega'} \tilde{\boldsymbol{V}}^{\rm t} n_i \left(\boldsymbol{K}_{ij}\frac{\partial}{\partial x_j}(\boldsymbol{U}_h+\tilde{\boldsymbol{U}}) - \boldsymbol{A}_i^{\rm f}(\boldsymbol{U}_h+\tilde{\boldsymbol{U}}) \right) {\rm d}\Gamma \\ + \int_{\Omega'} \tilde{\boldsymbol{V}}^{\rm t} \mathcal{L}(\boldsymbol{U}_{0,h};\tilde{\boldsymbol{U}})\,{\rm d}\Omega = \int_{\Omega'} \tilde{\boldsymbol{V}}^{\rm t}\left[\boldsymbol{F} - \mathcal{L}(\boldsymbol{U}_{0,h};\boldsymbol{U}_h)\right]{\rm d}\Omega, \end{aligned} \tag{27}$$

where n_i is the i-th component of the exterior normal to $\partial\Omega$ and $\mathcal{L}^*$ is the adjoint operator of $\mathcal{L}$ with homogeneous Dirichlet conditions.

Equation (27) is equivalent to finding $\tilde{\boldsymbol{U}} \in \tilde{\mathcal{W}}$ such that

$$\mathcal{L}(\boldsymbol{U}_{0,h};\tilde{\boldsymbol{U}}) = \boldsymbol{F} - \mathcal{L}(\boldsymbol{U}_{0,h};\boldsymbol{U}_h) + \boldsymbol{V}_{h,\rm ort} \quad \text{in } \Omega^e, \tag{28}$$

$$\tilde{\boldsymbol{U}} = \tilde{\boldsymbol{U}}_{\rm ske} \quad \text{on } \partial\Omega^e, \tag{29}$$

for $e = 1, ..., n_{\rm el}$, where $\boldsymbol{V}_{h,\rm ort}$ is obtained from the condition that $\tilde{\boldsymbol{U}}$ must belong to $\tilde{\mathcal{W}}$ (and not to the whole space $\mathcal{W}$) and $\tilde{\boldsymbol{U}}_{\rm ske}$ is a function defined on the element boundaries and such that

$$\boldsymbol{q}_n := n_i \left(\boldsymbol{K}_{ij}\frac{\partial}{\partial x_j}(\boldsymbol{U}_h+\tilde{\boldsymbol{U}}) - \boldsymbol{A}_i^{\rm f}(\boldsymbol{U}_h+\tilde{\boldsymbol{U}}) \right) \tag{30}$$

is continuous across interelement boundaries, that is to say, the normal component of the fluxes of $\boldsymbol{U}$ is continuous across these boundaries. Observe that due to this fact the first term in the LHS of (27) vanishes. We call $\tilde{\boldsymbol{U}}_{\rm ske}$ the skeleton of $\tilde{\boldsymbol{U}}$.

Problem (23)-(24) is exactly equivalent to (26)-(28)-(29). The approximate problem is defined by the way in which problem (28)-(29) is solved as well as by the way in which the functions $\boldsymbol{V}_{h,\rm ort}$ and $\tilde{\boldsymbol{U}}_{\rm ske}$ are taken. A particularly simple case is described next. However, this point can be further exploited, as suggested in a previous work[21] where, in particular, the subscales are taken orthogonal to the finite element space.

3.2.2 Algebraic approximation to the subscales

The simplest way to approximate problem (28)-(29) is to take

$$\tilde{\boldsymbol{U}} \approx \boldsymbol{\tau}\left[\boldsymbol{F} - \mathcal{L}(\boldsymbol{U}_{0,h}; \boldsymbol{U}_h)\right], \tag{31}$$

as the solution of this problem, where $\boldsymbol{\tau}$ is a $n_{\rm unk} \times n_{\rm unk}$ matrix defined within each element domain that has to be determined. We shall refer to it as the matrix of stabilization parameters. The approximation given by (31) has an implicit assumption on the function $\tilde{\boldsymbol{U}}_{\rm ske}$ and the space $\tilde{\mathcal{W}}$, and therefore on the function $\boldsymbol{V}_{h,\rm ort}$. In general, $\tilde{\boldsymbol{U}}$ will be discontinuous across interelement boundaries, so that the fluxes given by (30) will not even be well defined. However, from (26) it is observed that, except for the boundary integral, only the component of $\tilde{\boldsymbol{U}}$ in $\mathcal{L}(\boldsymbol{U}_{0,h}; \mathcal{W}_h)$ is needed, where $\mathcal{L}(\boldsymbol{U}_{0,h}; \mathcal{W}_h)$ is the space of functions of the form $\mathcal{L}(\boldsymbol{U}_{0,h}; \boldsymbol{V}_h)$, with $\boldsymbol{V}_h \in \mathcal{W}_h$. We may think of (31) as the approximation to this component.

To close the approximation, we neglect the interelement boundary terms in (26), so that the problem that has to be solved is finally

$$B(\boldsymbol{U}_{0,h}; \boldsymbol{U}_h, \boldsymbol{V}_h) + \int_{\Omega'} \tilde{\boldsymbol{U}}^{\rm t} \mathcal{L}^*(\boldsymbol{U}_{0,h}; \boldsymbol{V}_h)\, {\rm d}\Omega \;\; = \;\; L(\boldsymbol{V}_h), \tag{32}$$

with $\tilde{\boldsymbol{U}}$ given by (31). With all these assumptions we have arrived to a method proposed previously[20] using different arguments. In particular, (31) was derived from an approximation to the Green's function of the problem. This method was also considered in the literature[22] and derived for the scalar diffusion-reaction equation by using bubble functions.[23]

The way to compute matrix $\boldsymbol{\tau}$ is general situations is still not clear. Traditionally, the way to proceed has been to obtain particular expressions for simplified problems and then to extend it to more complex situations. Very often, the appropriateness of the expressions thus obtained have been confirmed by convergence analyses.

In the numerical example presented in Section 4, we have employed a simple approximation for $\boldsymbol{\tau}$[21] (in the two dimensional case):

$$\boldsymbol{\tau} = {\rm diag}(\tau_1, \tau_1, \tau_2, \tau_3), \tag{33}$$

where

$$\tau_1 = \left[c_1 \frac{\mu}{h^2} + c_2 \frac{\rho|\boldsymbol{u}_{0,h}|}{h}\right]^{-1}, \quad \tau_2 = \frac{h^2}{c_1 \tau_1}, \quad \tau_3 = \left[c_1 \frac{k}{h^2} + c_2 \frac{\rho|\boldsymbol{u}_{0,h}|}{h}\right],$$

where c_1 and c_2 are algorithmic constants that we take $c_1 = 4$ and $c_2 = 2$ for linear elements and $\boldsymbol{u}_{0,h}$ is the velocity component of $\boldsymbol{U}_{0,h}$.

This concludes the description of the stabilized finite element method we use and that is very similar to the formulation used by other authors in the same context.[24,25] Nevertheless, several points could be further analyzed, such as the subscale approximation in nonlinear problems,[21] the possibility of taking the space for the subscales orthogonal to the finite element space[21] or the use of a nondiagonal expression for $\boldsymbol{\tau}$, which in particular could account for the instabilities arising in strongly coupled problems.

3.3 Linearization

In the presentation of the stabilized finite element method we have considered that $\boldsymbol{U}_{0,h}$ was given. Since our problem is nonlinear, it is in fact a given guess for the unknown $\boldsymbol{U}_h$, from which we want to compute the next iterate. Therefore, in the development of the stabilization terms we have considered a sort of fixed point iteration. However, for the operator $\mathcal{L}(\boldsymbol{U};\boldsymbol{U})$ we consider several possibilities of linearization, all of which can be written in a compact form by making use of the linearized matrices of the system viewed as a nonlinear convection-diffusion-reaction equation.

Let $\lambda_{i,j}$ a collection of numbers that can take only the values 0 and 1. For $i=1$ we will use them to write the linearized momentum equation, for $i=2$ the continuity equation and for $i=3$ the energy equation. If $\boldsymbol{U}^{k-1}$ is the iterate $k-1$ of the unknown $\boldsymbol{U}$ (from which we wish to compute $\boldsymbol{U}^k$) the matrices of the linearized operator we consider are:

Low Mach number model:

$$\boldsymbol{A}_i^{\rm lin}(\boldsymbol{U}^{k-1}) = \begin{bmatrix} \rho^{k-1}u_i^{k-1} & 0 & \delta_{i1} & 0 \\ 0 & \rho^{k-1}u_i^{k-1} & \delta_{i2} & 0 \\ \delta_{i1} & \delta_{i2} & 0 & -\frac{\lambda_{21}}{\theta^{k-1}}u_i^{k-1} \\ 0 & 0 & 0 & \rho^{k-1}u_i^{k-1} \end{bmatrix},$$

$$\boldsymbol{S}^{\rm lin}(\boldsymbol{U}^{k-1}) = \begin{bmatrix} \lambda_{11}\rho^{k-1}\partial_1 u_1^{k-1} & \lambda_{11}\rho^{k-1}\partial_2 u_1^{k-1} & 0 & \frac{\rho^{k-1}}{\theta^{k-1}}\left(-\lambda_{12}\boldsymbol{u}^{k-1}\cdot\nabla u_1^{k-1}+\lambda_{13}g_1\right) \\ \lambda_{11}\rho^{k-1}\partial_1 u_2^{k-1} & \lambda_{11}\rho^{k-1}\partial_2 u_2^{k-1} & 0 & \frac{\rho^{k-1}}{\theta^{k-1}}\left(-\lambda_{12}\boldsymbol{u}^{k-1}\cdot\nabla u_2^{k-1}+\lambda_{13}g_2\right) \\ -\frac{\lambda_{22}}{\theta^{k-1}}\partial_1\theta^{k-1} & -\frac{\lambda_{22}}{\theta^{k-1}}\partial_2\theta^{k-1} & 0 & \frac{\lambda_{23}}{(\theta^{k-1})^2}\boldsymbol{u}^{k-1}\cdot\nabla\theta^{k-1} \\ \lambda_{31}\rho^{k-1}\partial_1\theta^{k-1} & \lambda_{31}\rho^{k-1}\partial_2\theta^{k-1} & 0 & -\frac{\rho^{k-1}}{\theta^{k-1}}\lambda_{32}\boldsymbol{u}^{k-1}\cdot\nabla\theta^{k-1} \end{bmatrix},$$

$$\boldsymbol{F}^{\rm lin}(\boldsymbol{U}^{k-1}) = \begin{bmatrix} (-\lambda_{11}+\lambda_{12})\rho^{k-1}\boldsymbol{u}^{k-1}\cdot\nabla u_1^{k-1}+(1+\lambda_{13})\rho^{k-1}g_1 \\ (-\lambda_{11}+\lambda_{12})\rho^{k-1}\boldsymbol{u}^{k-1}\cdot\nabla u_2^{k-1}+(1+\lambda_{13})\rho^{k-1}g_2 \\ (1-\lambda_{21}-\lambda_{22}+\lambda_{23})\frac{1}{\theta^{k-1}}\boldsymbol{u}^{k-1}\cdot\nabla\theta^{k-1} \\ (-\lambda_{31}+\lambda_{32})\rho^{k-1}\boldsymbol{u}^{k-1}\cdot\nabla\theta^{k-1}+Q \end{bmatrix}.$$

The parameters λ_{11} and λ_{12} correspond to the linearization of the convective term in the momentum equation ($\lambda_{11}=\lambda_{12}=1$ would be Newton's method, whereas other options would be fixed point methods), whereas λ_{13} is used to decide whether the buoyancy term is treated in a coupled or in a block iterative way. Likewise, λ_{2j}, $j=1,2,3$, determine both the linearization of the term $(1/\theta)\boldsymbol{u}\cdot\nabla\theta$ ($\lambda_{2j}=1$ would be full Newton's method) and the possibility to treat this term in a staggered way ($\lambda_{2j}=0$). Finally, λ_{3j}, $j=1,2$, play the same role for the energy equation as λ_{1j}, $j=1,2$, for the momentum equation.

Boussinesq model:

$$\boldsymbol{A}_i^{\rm lin}(\boldsymbol{U}^{k-1}) = \begin{bmatrix} \rho u_i^{k-1} & 0 & \delta_{i1} & 0 \\ 0 & \rho u_i^{k-1} & \delta_{i2} & 0 \\ \delta_{i1} & \delta_{i2} & 0 & 0 \\ 0 & 0 & 0 & \rho u_i^{k-1} \end{bmatrix},$$

$$\boldsymbol{S}^{\rm lin}(\boldsymbol{U}^{k-1}) = \begin{bmatrix} \lambda_{11}\rho\partial_1 u_1^{k-1} & \lambda_{11}\rho\partial_2 u_1^{k-1} & 0 & \lambda_{12}\rho\beta g_1 \\ \lambda_{11}\rho\partial_1 u_2^{k-1} & \lambda_{11}\rho\partial_2 u_2^{k-1} & 0 & \lambda_{12}\rho\beta g_2 \\ 0 & 0 & 0 & 0 \\ \lambda_{31}\rho\partial_1\theta^{k-1} & \lambda_{31}\rho\partial_2\theta^{k-1} & 0 & 0 \end{bmatrix},$$

$$\boldsymbol{F}^{\rm lin}(\boldsymbol{U}^{k-1}) = \begin{bmatrix} \lambda_{11}\rho\boldsymbol{u}^{k-1}\cdot\nabla u_1^{k-1} - (1-\lambda_{12})\rho\beta g_1\theta^{k-1} + \rho\beta\theta_0 g_1 \\ \lambda_{11}\rho\boldsymbol{u}^{k-1}\cdot\nabla u_2^{k-1} - (1-\lambda_{12})\rho\beta g_1\theta^{k-1} + \rho\beta\theta_0 g_2 \\ 0 \\ \lambda_{31}\rho\boldsymbol{u}^{k-1}\cdot\nabla\theta^{k-1} + Q \end{bmatrix}.$$

The meaning of the parameters λ_{ij} is similar to the previous case.

With these matrices we can define the linearized operator

$$\mathcal{L}^{\rm lin}(\boldsymbol{U}^{k-1};\boldsymbol{U}^k) := \boldsymbol{A}_i^{\rm lin}(\boldsymbol{U}^{k-1})\frac{\partial\boldsymbol{U}^k}{\partial x_i} - \frac{\partial}{\partial x_i}\left(\boldsymbol{K}_{ij}\frac{\partial\boldsymbol{U}^k}{\partial x_j}\right) + \boldsymbol{S}^{\rm lin}(\boldsymbol{U}^{k-1})\boldsymbol{U}^k,$$

as well as the linear forms associated to the linearization

$$B^{\rm lin}(\boldsymbol{U}^{k-1};\boldsymbol{U}^k,\boldsymbol{V}) := \langle \boldsymbol{V}^{\rm t}, \mathcal{L}^{\rm lin}(\boldsymbol{U}^{k-1};\boldsymbol{U}^k)\rangle,$$
$$L^{\rm lin}(\boldsymbol{U}^{k-1};\boldsymbol{V}) := \int_\Omega \boldsymbol{V}^{\rm t}\boldsymbol{F}^{\rm lin}\,{\rm d}\Omega + \int_{\Gamma_N}\boldsymbol{V}^{\rm t}\boldsymbol{T}\,{\rm d}\Gamma,$$

which allow us to write the fully discrete and linearized problem as

$$B^{\rm lin}(\boldsymbol{U}_h^{k-1};\boldsymbol{U}_h^k,\boldsymbol{V}_h) - \int_{\Omega'}\mathcal{L}^*(\boldsymbol{U}_h^{k-1};\boldsymbol{V}_h)\boldsymbol{\tau}^{k-1}\mathcal{L}^{\rm lin}(\boldsymbol{U}_h^{k-1};\boldsymbol{U}_h^k)\,{\rm d}\Omega$$
$$= L^{\rm lin}(\boldsymbol{U}_h^{k-1};\boldsymbol{V}_h) + \int_{\Omega'}\mathcal{L}^*(\boldsymbol{U}_h^{k-1};\boldsymbol{V}_h)\boldsymbol{\tau}^{k-1}\boldsymbol{F}^{\rm lin}\,{\rm d}\Omega.$$

The superscript $k-1$ in $\boldsymbol{\tau}^{k-1}$ has been used to indicate that the matrix is computed with the unknown of iteration $k-1$.

Finally, in some cases we have found convenient to use a relaxation scheme of the form

$$\boldsymbol{U}_h^k \leftarrow \alpha\boldsymbol{U}_h^k + (1-\alpha)\boldsymbol{U}_h^{k-1}, \tag{34}$$

with the relaxation parameter $0 < \alpha \leq 1$. We have not implemented any particular algorithm to seek an optimal value of α. A case with $\alpha = 0.5$ will be shown in the following Section.

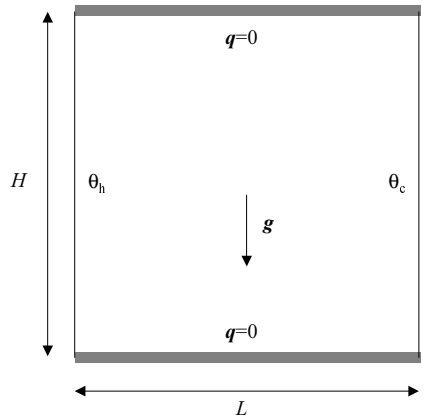

Figure 1: Geometry and boundary conditions of the problem

4 NUMERICAL EXAMPLE

The natural convection in a cavity is a standard benchmark for numerical methods on thermally coupled flows. It was initially devised for Boussinesq flows[26] and later for low Mach number flows.[27] The problem is sketched in Figure 1.

First of all, let us mention the conditions for the validity of the approximations in this example. As this is a natural convection problem, a velocity scale must be chosen. Taking for example the viscous scale and using the benchmark specifications[27] gives a Mach number of 2.2×10^{-5}, allowing the use of the zero Mach number equations. The conditions of applicability of the Boussinesq approximation need some care. As shown in the derivation, the zeroth order temperature and density must be functions of the vertical coordinate only or must be constants. In order to have this reference state, the (dimensionless) temperature difference between vertical walls must vanish. Finally, the Boussinesq number must tend to zero as fast as the Mach number (what is a restriction of the vertical scale of the problem). In the conditions of the benchmark, the Boussinesq number is 5.7×10^{-5} and is of the same order as the Mach number. Thus, the dimensionless parameters that define the problem are

$$\varepsilon = \frac{T_h - T_c}{T_h + T_c}, \quad A = \frac{H}{L}, \quad Pr = \frac{c_p \mu}{k}, \quad Ra = PrGr = Pr\frac{gL^3}{\nu^2}\varepsilon,$$

where Pr is the Prandtl number, Ra the Rayleigh number and Gr the Grashof number.

Let us start by trying to get some physical insight on the effect of the temperature difference between the walls of the cavity, and therefore on the validity of the Boussinesq approximation. In Figure 2 we plot the streamlines and temperature contours for different values of ε at $Ra = 10^6$. It is observed that whereas the temperature contours do not change significantly, there is a noticeable change in the flow pattern.

For $Ra = 10^3$ there is a single central vortex instead of the three appearing in Figure 2. This central vortex moves to the right as ε is increased. This effect is quantified in Table 1 . It is

observed that the error that would be made in the vortex position using the Boussinesq model would be of the order of the 27%.

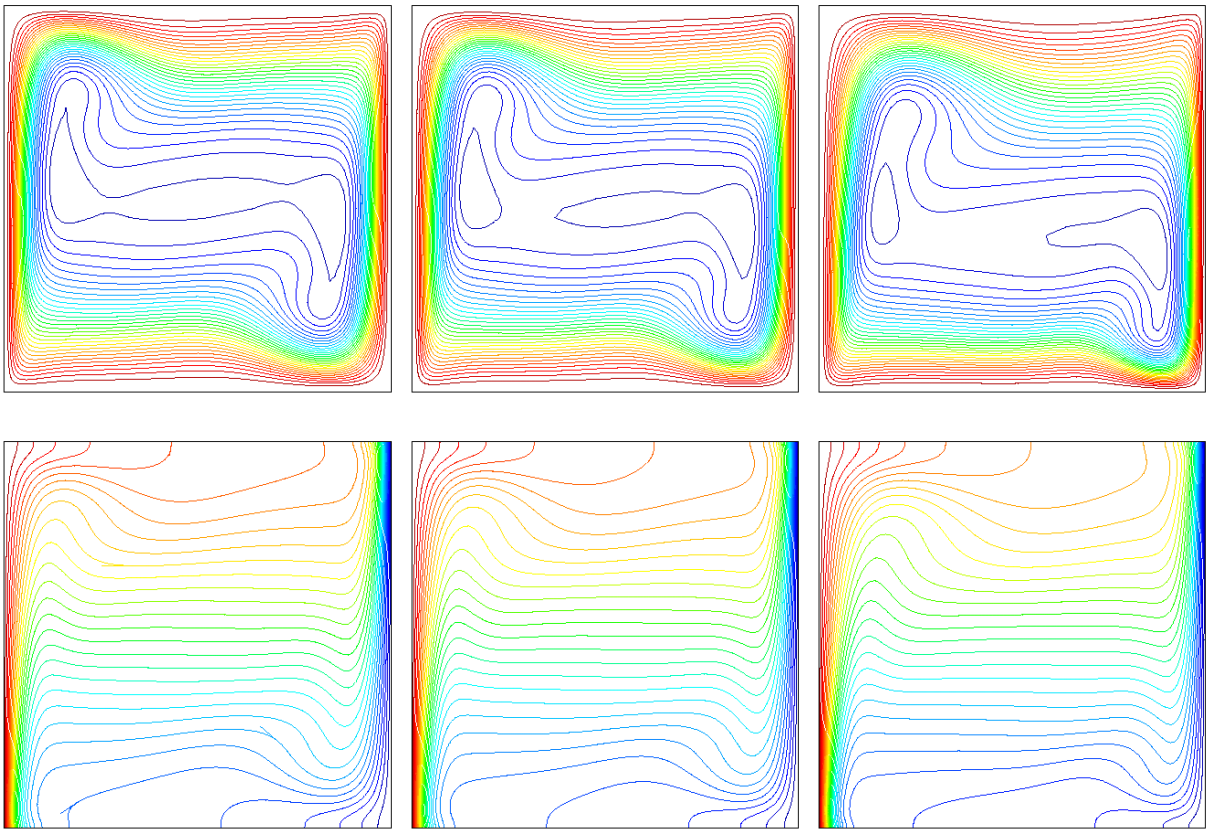

Figure 2: Streamlines (top) and temperature contours (bottom) at $Ra = 10^6$ for the low Mach number model. From the left to the right: $\varepsilon = 0.005$, 0.2 and 0.6

The change in the Nusselt number distribution with ε along the hot wall at $Ra = 10^3$ and 10^5 is shown in Figure 3. The average Nusselt number does not change much, but some changes can be observed in its distribution.

Let us move now to numerical aspects. First, we have studied the convergence in h of the average Nusselt number. We have used structured meshes of bilinear elements refined near the walls, with a number of elements per direction ranging from $N = 10$ to $N = 80$. Results are shown in Table 2, where $h := 1/N$. The reference values, taken from the literature,[25,26,28] have been obtained with very fine discretizations. The classical convergence plot is shown in Figure 4 in two particular cases. From these results it is seen that h convergence is increasingly difficult with ε, although in all the cases presented the behavior is as expected.

An aspect that is particularly relevant in our problem is the convergence of the iterative scheme. From the convergence plots shown in Figures 5 to 7 several conclusions can be drawn. First (Figures 5 and 7) it is clear that it is convenient to treat in a fully coupled way the buoyancy forces and to use a Newton linearization *at least for the convective term of the energy equation*,

ε	x coordinate
0.0	0.500
0.005	0.500
0.01	0.500
0.13	0.525
0.2	0.549
0.4	0.573
0.6	0.638

Table 1: Evolution of the x-coordinate of the central vortex for $Ra = 10^3$ in terms of ε

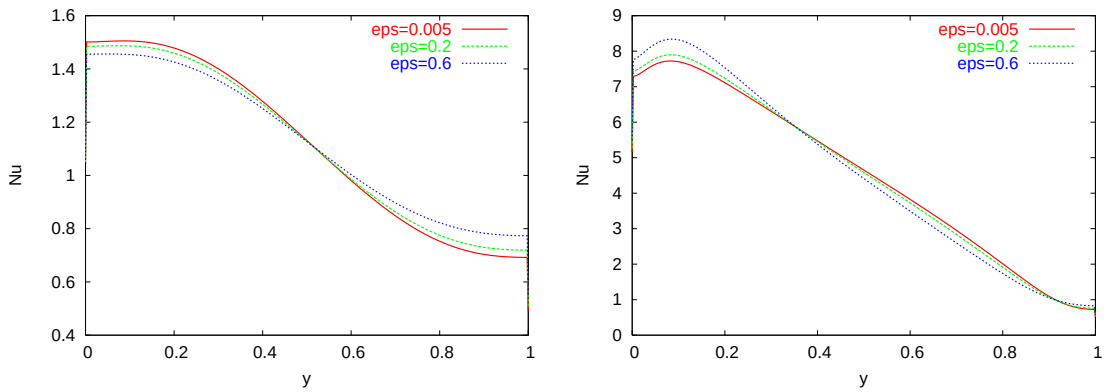

Figure 3: Nusselt number distribution along the hot wall. From the left to the right: $Ra = 10^3$ and 10^5.

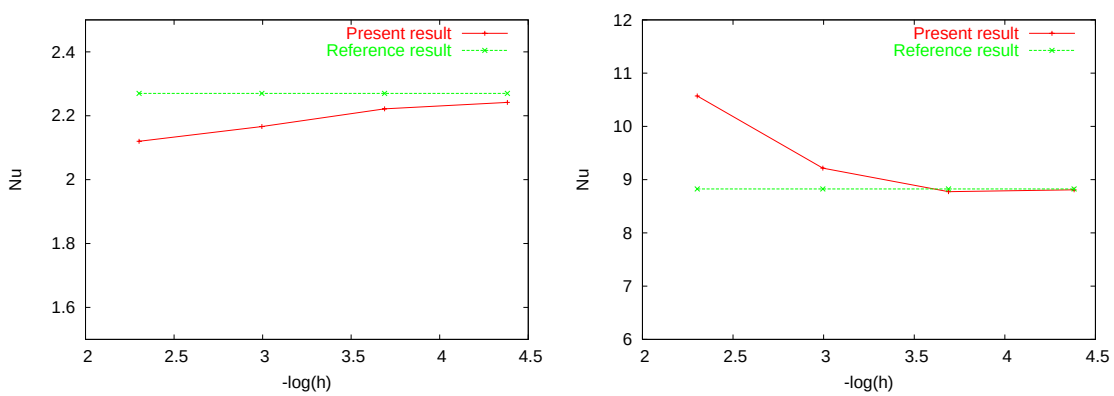

Figure 4: h convergence of the Nusselt number for $\varepsilon = 0.6$ compared to reference results.[28] From the left to the right: $Ra = 10^4$ and 10^6.

h	$Ra = 10^3$	$Ra = 10^4$	$Ra = 10^5$	$Ra = 10^6$
Boussinesq				
0.1000	0.1102501E+01	0.2185881E+01	0.4441898E+01	0.8363745E+01
0.0500	0.1114341E+01	0.2226975E+01	0.4483480E+01	0.8719423E+01
0.0250	0.1117034E+01	0.2240036E+01	0.4510844E+01	Not converged
0.0125	0.1117617E+01	0.2243569E+01	0.4518729E+01	0.8820067E+01
Reference[26]	0.118E+01	0.2243E+01	0.4519E+01	0.88E+01
$\varepsilon = 0.005$				
0.1000	0.1101139E+01	0.2222317E+01	0.4637871E+01	0.9212141E+01
0.0500	0.1113684E+01	0.2229419E+01	0.4503834E+01	0.8872408E+01
0.0250	0.1116842E+01	0.2239957E+01	0.4512237E+01	0.8816794E+01
0.0125	0.1117568E+01	0.2243493E+01	0.4518754E+01	0.8820836E+01
Reference[26]	0.118E+01	0.2243E+01	0.4519E+01	0.88E+01
$\varepsilon = 0.2$				
0.1000	0.1098962E+01	0.2202645E+01	0.4713655E+01	0.9458602E+01
0.0500	0.1112939E+01	0.2218412E+01	0.4495775E+01	0.8924234E+01
0.0250	0.1117119E+01	0.2236924E+01	0.4507990E+01	0.8805386E+01
0.0125	0.1118204E+01	0.2243379E+01	0.4520072E+01	0.8817329E+01
$\varepsilon = 0.4$				
0.1000	0.1096073E+01	0.2173146E+01	0.4823505E+01	0.1015805E+02
0.0500	0.1112693E+01	0.2200920E+01	0.4486731E+01	0.9011334E+01
0.0250	0.1118633E+01	0.2232650E+01	0.4505211E+01	0.8795187E+01
0.0125	0.1120302E+01	0.2244016E+01	0.4526855E+01	0.8817175E+01
$\varepsilon = 0.6$				
0.1000	0.1090356E+01	0.2120140E+01	0.5030137E+01	0.1057136E+02
0.0500	0.1111590E+01	0.2166190E+01	0.4465701E+01	0.9215231E+01
0.0250	0.1120820E+01	0.2221468E+01	0.4492835E+01	0.8774527E+01
0.0125	0.1123541E+01	0.2241822E+01	0.4532746E+01	0.8808319E+01
Reference[28]	-	0.2270E+01	-	0.8825E+01
Reference[25]	-	-	-	0.885978E+01

Table 2: h convergence of the Nusselt number

both for the Boussinesq and the low Mach number models. Likewise (Figure 6), some problems do not converge unless a relaxation scheme is employed (see (34)).

5 CONCLUSIONS

In this paper we have tried to introduce both the physical grounds of thermally coupled low speed flows and its numerical approximation. Concerning the physical model, we have pre-

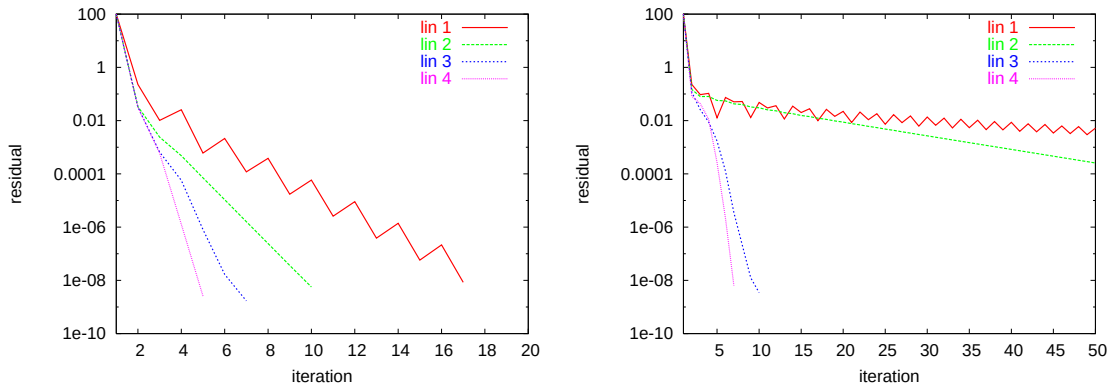

Figure 5: Non linear convergence of the Boussinesq model. From the left to the right: $Ra = 10^3$ and 10^4. **lin1**: $\lambda_{11} = 0, \lambda_{12} = 0, \lambda_{31} = 0$, **lin2**: $\lambda_{11} = 0, \lambda_{12} = 1, \lambda_{31} = 0$, **lin3**: $\lambda_{11} = 0, \lambda_{12} = 1, \lambda_{31} = 1$, **lin4**: $\lambda_{11} = 1, \lambda_{12} = 1, \lambda_{31} = 1$

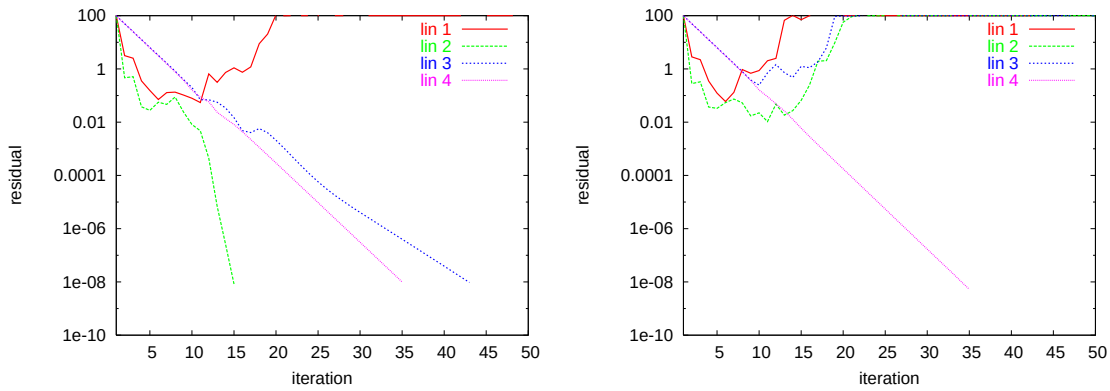

Figure 6: Non linear convergence of the Boussinesq model at $Ra = 10^6$. From the left to the right: meshes of 40×40 and of 80×80 elements. **lin1**: $\lambda_{11} = 0, \lambda_{12} = 1, \lambda_{31} = 1, \alpha = 1$ in (34), **lin2**: $\lambda_{11} = 1, \lambda_{12} = 1, \lambda_{31} = 1, \alpha = 1$ in (34), **lin3**: $\lambda_{11} = 0, \lambda_{12} = 1, \lambda_{31} = 1, \alpha = 0.5$ in (34), **lin4**: $\lambda_{11} = 1, \lambda_{12} = 1, \lambda_{31} = 1, \alpha = 0.5$ in (34)

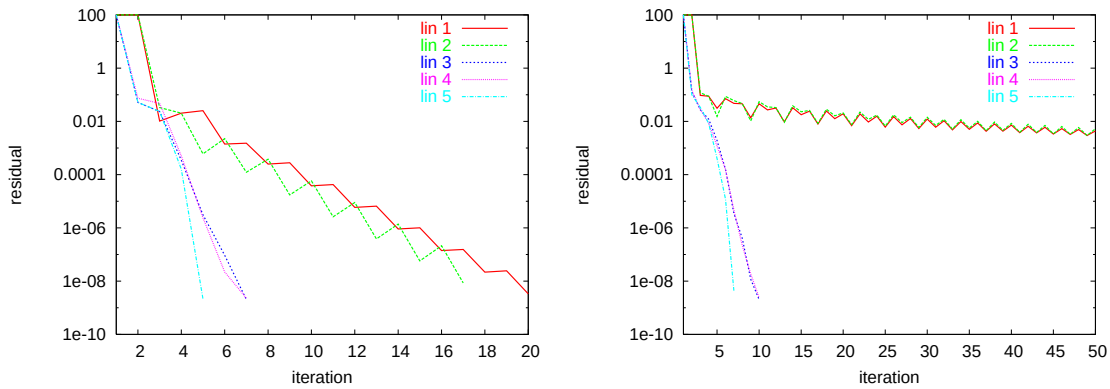

Figure 7: Non linear convergence of the Low Mach number model. From the left to the right: $Ra = 10^3$ and 10^4. **lin1**: all $\lambda_{ij} = 0$, **lin2**: $\lambda_{21} = 1$, rest of $\lambda_{ij} = 0$, **lin3**: $\lambda_{21} = 1$, $\lambda_{31} = 1$, rest of $\lambda_{ij} = 0$, **lin4**: $\lambda_{21} = 1$, $\lambda_{31} = 1$, $\lambda_{22} = 1$, rest of $\lambda_{ij} = 0$, **lin5**: all $\lambda_{ij} = 1$

sented an asymptotic analysis that allows to derive the classical zero Mach number limit equations from the general compressible flow equations, as well as to understand the assumptions on which the Boussinesq model relies.

From the numerical viewpoint, the stabilized finite element formulation we have presented has proved to be free of numerical instabilities and accurate, yielding quite acceptable errors on rather coarse meshes. In what concerns the linearization of the equations, we have found that it is important to treat bouyancy forces fully coupled with the momentum equation (not in a staggered way) and linearize to second order (Newton's method) at least the convective term in the energy equation. Relaxation has also proven to be effective in some cases, athough no attempt has been made to choose the optimal relaxation parameter.

REFERENCES

[1] R. G. Rehm and H. R. Baum. The equations of motion for thermally driven bouyant flows. *Journal of research of the National Bureau of Standards*, **83**(3), 297–308 (1978).

[2] S. Paolucci. On the filtering of sound from the Navier-Stokes equations. Technical Report 82-8257, Sandia National Laboratories, (1982).

[3] A. Majda and J. Sethian. The derivation and numerical solution of the equations for zero Mach number combustion. *Combustion science and technology*, **42**, 185–205 (1985).

[4] R. Klein, N. Botta, T. Schneider, C. D. Munz, S. Roller, A. Meister, L. Hoffmann, and T. Sonar. Asymptotic adaptive methods for multi-scale problems in fluid mechanics. *Journal of Engineering Mathematics*, **39**, 261–343 (2001).

[5] B. Müller. Low Mach number asymptotics of the Navier-Stokes equations. *Journal of Engineering Mathematics*, **34**, 97–109 (1998).

[6] E. A. Spiegel and G. Veronis. On the Boussinesq approximation for a compressible fluid. *Astrophysics Journal*, **131**, 442–447 (1960).

[7] John M. Mihaljan. A rigorous exposition of the Boussinesq approximations applicable to a thin layer of fluid. *Astrophysics Journal*, **136**(3), 1126–1133 (1962).

[8] R. Perez Cordon and M. G. Velarde. On the (non-linear) foundations of Boussinesq approximation applicable to a thin-layer of fluid. *Journal de physique*, **36**(7), 591–601 (1975).

[9] D. D. Gray and A. Giorgini. The validity of the Boussinesq approximation for liquids and gases. *International Journal of Heat and Mass Transfer*, **19**(5), 545–551 (1976).

[10] R. Kh. Zeytounian. A rigoous derivation of the equations of compresible viscous fluid motion with gravity at low Mach number. *Archiwum Mechaniki Stosowanej*, **26**, 499–509 (1974).

[11] R. Kh. Zeytounian. *Asymptotic modelling of atmospheric flows*. Springer Verlag, Heidelberg, (1990).

[12] R. Kh. Zeytounian. Joseph Boussinesq and his approximation: a contemporary view. *Comptes Rendus Mecanique*, **331**(8), 575–586 (Aug 2003).

[13] P. A. Bois. Propagation linéare et non linéaire d'ondes atmosphériques. *Journal de Mécanique*, **15**(5), 781–811 (1976).

[14] P. A. Bois. Asymptotic aspects of the Boussinesq approximation for gases and liquids. *Geophysics and Astrophysics Fluid Dynamics*, **58**, 45–55 (1991).

[15] G. K. Batchelor. The conditions for dynamical similarity of motions of a frictionless perfect gas atmosphere. *Quarterly Journal of the Royal Meteorological Society*, **79**, 224–235 (1953).

[16] Y. Ogura and N. A. Phillips. Scale analysis of deep and shallow convection in atmosphere. *Journal of the atmospheric sciences*, **19**, 173–179 (1962).

[17] J. Kevorkian and J. D. Cole. *Perturbation Methods in Applied Mathematics*, volume 34 of *Applied mathematical sciences*. Springer-Verlag, New York, (1981).

[18] A. Meister. Asymptotic single and multiple scale expansions in the low Mach number limit. Technical report, Institut fur Angewandte Matematik Universitat Hamburg, (1998).

[19] M. S. Howe. *Acoustics of fluid-structure interactions*. Cambridge monographs on mechanics. Cambridge University Press, Cambridge, (1998).

[20] T.J.R. Hughes. Multiscale phenomena: Green's function, the Dirichlet-to-Neumann formulation, subgrid scale models, bubbles and the origins of stabilized formulations. *Computer Methods in Applied Mechanics and Engineering*, **127**, 387–401 (1995).

[21] R. Codina. Stabilized finite element approximation of transient incompressible flows using orthogonal subscales. *Computer Methods in Applied Mechanics and Engineering*, **191**, 4295–4321 (2002).

[22] L. Franca, S.L. Frey, and T.J.R. Hughes. Stabilized finite element methods: I. Application to the advective-diffusive model. *Computer Methods in Applied Mechanics and Engineering*, **95**, 253–276 (1992).

[23] L.P. Franca and C. Farhat. Bubble functions prompt unusual stabilized finite element methods. *Computer Methods in Applied Mechanics and Engineering*, **123**, 299–308 (1994).

[24] R. Becker and M. Braack. Solution of a stationary benchmark problem for natural convection with large temperature difference. *International Journal of Thermal Sciences*, **41**(5), 428–439 (Apr 2002).

[25] V. Heuveline. On higher-order mixed fem for low Mach number flows: application to a natural convection benchmark problem. *International Journal for Numerical Methods in Fluids*, **41**, 1339–1356 (2003).

[26] G. De Vahl Davis and I.P. Jones. Natural convection in a square cavity: a comparison exercise. *International Journal for numerical methods in fluids*, **3**, 227–248 (1983).

[27] P. Le Quéré and P. Paillère. Modelling and simulation of natural flows with large temperature differences: a benchmark problem for low Mach number solvers. In *Workshop/12th CFD seminar*, pages 14–22, France, (2000). CEA Saclay.

[28] M.J. Martinez and D.K. Gartling. A finite element method for low-speed compressible flows. *Computer Methods in Applied Mechanics and Engineering*, **193**(21-22), 1959–1979 (May 2004).